IJCRT.ORG ISSN : 2320-2882

INTERNATIONAL JOURNAL OF CREATIVE RESEARCH THOUGHTS (IJCRT)

An International Open Access, Peer-reviewed, Refereed Journal

Structure, Spectroscopy and Electronic Properties of 1,2,3, triazole pyrazoline hybrid: DFT and Experimental Approach

[1]Dinesh kumar Matheshwaran, [2]Pooja Shri Senthil kumar, [3]Krishanamoorthy Sundaram, [4,*]Ravikumar Raju

[1]Assistant professor, [2]PG Student, [3]Associate Professor, [4,*]Associate Professor

[1]Department of Chemistry,

[1]Dr.N.G.P Arts and Science College, Coimbatore, Tamil Nadu, India

Abstract: In the present work by using density functional theory, the structural parameters and properties of 4-methyl-1-(4-nitrophenyl)-5-5-(2-nitrophenyl)-4-5-dihydro-1H1,2,3 triazole has been confirmed. Optimum geometries, vibration spectra and NMR spectra of 4-methyl-1-(4-nitrophenyl)-5-5-(2-nitrophenyl)-4-5-dihydro-1H1,2,3 triazole (4M4N2NT) were predicted by DFT computations at B3LYP using 6–311++ G(d, p) and 6-31Gbasis functions. IR spectrum was evaluated mathematically and qualitatively by considering PED across individual vibrating mode. Stretching, bending, deformation and vibration, and are examined through chemcraft. 1H and 13C NMR NMR graph is based on SCF GIAO magnetic shielding method are plotted through Gaussian 09W software. In light of Hyperpolarizability values, NLO functionality was investigated and it was discovered that 4M4N2NT could serve to be suitable NLO element.

Index Terms – DFT, IR, NMR, NLO, NBO, ESP, 1,2,3 - trizole pyrazoline hybrid

I. INTRODUCTION

The pyrazoline is the dihydro derivative of pyrazole (1). Pyrazoline is a five membered ring and are known as dihydropyrazolene (2-3). The pyrazoline compound has one endocyclic bond within the ring, along with two adjacent nitrogen atom and they are electron rich nitrogenous heterocycles (3). The nitrogen carrying pyrazoline plays an important role in diverse pharmaceutical action as drugs and the N-N bond linkage in pyrazoline ring are responsible for their biological action (4). Pyrazoline derivatives possess anti-microbial activity is one of the important pharmaceutical properties (5). The pyrazoline compounds are not stable and are readily converted to cyclopropane derivative in presence of basic catalyst (6). To observe enhancement in the therapeutic behavior the pyrazoline moiety was linked with 1,2,3-triazole an yet another important bioactive molecule. Theoretical and experimental value for the synthesized triazole pyrazoline hybrid was carried out to perceive the electronic, magnetic, vibrational, and structural properties of molecule using documented FT-IR, NMR spectra with the DFT quantum computational theories with the appropriate basic set (7-8). The time-dependent density functional theory was employed by using B3LYP exchange co-relation functional and 6-311++G (d, p) basic set (9-10).

II. Experimental details:

The 4-methyl-1-(4-nitrophenyl)-5-5-(2-nitrophenyl)-4-5-dihydro-1H1,2,3 triazole (compound A) was synthesized by the reaction of chalcone with hydrazine hydrate and the reaction is monitored by thin layer chromatography. The pure pyrazoline compound was characterized by IR, ^{1}H NMR, ^{13}C NMR and EI mass spectroscopy. The IR analysis was documented on Perkin - Elmer model 1620 FT-IR spectrophotometer. The mass spectra of the pyrazoline compounds was documented on a JEOL mass spectrometer. ^{1}H NMR and ^{13}C NMR are recorded using deuterated dimethyl sulfoxide (DMSO) solvent on Brucker Avance high resolution nuclear magnetic resonance spectrophotometer (300 MHz).

III. Computational details:

The quantum chemical calculation was carried out for the pyrazoline compound A using density functional theory with Becke3-Lee-Yang-Parr (B3LYP) as hybrid functional and is combined with the 631+G and 6311+G (d, p) basic set using GAUSSIAN 09 program package. Primarily the molecular geometry optimization was done followed by the properties such as vibrational analysis, NMR, Frontier molecular orbital analysis, Contour, and total density, Mullikan charges and Electrostatic potential. It was proved that there are no negative wave number in these computed values after the optimization analysis. The vibration analysis and electronic transition value are pictured by the Chemcraft program.

3.1 Geometric structural parameters:

The optimized geometrical parameters such as the bond angle and bond length were performed by DFT/B3LYP functional level with 6-311++G (d, p) and 6-31+ G basic sets. The optimized structure of 4M4N2NT with its optimized values of bond angle and bond length are presented in Table 1.

In 4M4N2NT, the bond length of NO_2 in fourth position are N7-08 in 631G are 1.2306 and N7-O9 are 1.2304, the other NO_2 in second position N27-O28 and N27-029 are 1.2334 and 1.2268. For the 1,2,3 triazole ring, the N10-N11 and N11-N12 are 1.3692 and 1.2974. The bond length of the N18-H37 is 1.0124. The bond angle for N10-N11-N12 is 107.3384, O8-N9-O9 is 124.7999 and O28-N27-O29 is 124.7205.

Table 1. Optimized Geometrical Parameters of 4M4N2NT

Parameters	Methods (B3LYP)		Parameters	Methods (B3LYP)	
	6-31G	6-311G		6-31G	6-311G
Bond length(A^0)			Bond angle(^{0})		
C1-C2	1.3895	1.3869	C2-C1-C6	118.9608	119.0428
C1-C6	1.3941	1.3914	C2-C1-H30	121.5676	121.4669
C1-H30	1.0825	1.0808	C6-C1-H30	119.4692	119.4877
C2-C3	1.4008	1.3985	C1-C2-C3	119.6811	119.7084
C2-H31	1.0831	1.0811	C1-C2-H31	121.0837	121.1088
C3-C4	1.4011	1.3985	C3-C2-H31	119.2336	119.1794
C3-N10	1.4166	1.4157	C2-C3-C4	120.7073	120.6227
C4-C5	1.3906	1.3882	C2-C3-N10	118.7805	118.8337
C4-H32	1.0842	1.0823	C4-C3-N10	120.4544	120.5068
C5-C6	1.3934	1.3905	C3-C4-C5	119.7291	119.7376
C5-H33	1.0825	1.0809	C3-C4-H32	119.9072	119.9709
C6-N7	1.4709	1.4775	C5-C4-H32	120.3444	120.2762
N7-O8	1.2308	1.2241	C4-C5-C6	118.8667	118.973
N7-O9	1.2304	1.2233	C4-C5-H33	121.6094	121.5558
N10-N11	1.3692	1.3648	C6-C5-H33	119.514	119.4624
N10-C14	1.3776	1.3775	C1-C6-C5	122.0311	121.8964
N11-N12	1.2974	1.2921	C1-C6-N7	119.0408	119.1313
N12-C13	1.3656	1.3653	C5-C6-N7	118.9277	118.9713
C13-C14	1.3914	1.3861	C6-N7-O8	117.5884	117.5221
C13-C15	1.4921	1.4911	C6-N7-O9	117.6114	117.555
C14-C16	1.4533	1.4553	O8-N7-O9	124.7999	124.9227

C15-H34	1.0937		1.0914		C3-N10-N11	118.1963		118.5085
C15-H35	1.0919		1.0905		C3-N10-C14	131.0863		130.9632
C15-H36	1.0949		1.0935		N11-N10-C14	110.3066		110.1349
C16-N17	1.2953		1.2869		N10-N11-N12	107.3384		107.504
C16-C20	1.5225		1.5242		N11-N12-C13	110.2796		110.2945
N17-N18	1.3798		1.3664		N12-C13-C14	108.2841		108.1708
N18-C19	1.4667		1.4815		N12-C13-C15	122.003		122.0609
N18-H37	1.0124		1.0095		C14-C13-C15	129.6998		129.7536
C19-C20	1.5584		1.559		N10-C14-C13	103.7906		103.8953
C19-C21	1.5425		1.5233		N10-C14-C16	126.1846		125.912
C19-H38	1.0937		1.0928		C13-C14-C16	129.5861		129.8443
C20-H39	1.0953		1.0905		C13-C15-H34	111.4274		110.9782
C20-H40	1.0917		1.0911		C13-C15-H35	109.3227		109.1583
C21-C22	1.4033		1.4019		C13-C15-H36	111.3121		111.1681
C21-C26	1.4062		1.3999		H34-C15-H35	109.3604		109.498
C22-C23	1.3989		1.3904		H34-C15-H36	106.8196		107.512
C22-N27	1.478		1.4792		H35-C15-H36	108.5206		108.4726
C23-C24	1.3882		1.3895		C14-C16-N17	120.557		120.4383
C23-H41	1.0837		1.0822		C14-C16-C20	127.4174		125.6987
C24-C25	1.3956		1.3915		N17-C16-C20	111.8665		113.2959
C24-H42	1.0848		1.083		C16-N17-N18	108.9555		109.9317
C25-C26	1.3908		1.3918		N17-N18-C19	110.5264		112.7622
C25-H43	1.0854		1.0836		N17-N18-H37	111.5552		113.9919
C26-H44	1.087		1.0845		C19-N18-H37	117.473		120.7442
N27-O28	1.2334		1.2219		N18-C19-C20	99.7207		101.8689
N27-O29	1.2268		1.224		N18-C19-C21	119.6366		114.9739
N27-H37	2.5898		2.5967		N18-C19-H38	109.1802		107.7549
O28-H37	1.9897		1.9997		C20-C19-C21	111.244		117.8761
					C20-C19-H38	110.4068		108.6888
					C21-C19-H38	106.4729		105.2981
					C16-C20-C19	100.3222		101.6173
					C16-C20-H39	111.0471		113.0475
					C16-C20-H40	113.8237		110.4083
					C19-C20-H39	110.0442		110.5031
					C19-C20-H40	113.5522		113.1902
					H39-C20-H40	107.9401		108.0821
					C19-C21-C22	129.8749		126.0303
					C19-C21-C26	114.3332		117.914
					C22-C21-C26	115.5252		115.9183
					C21-C22-C23	122.5696		122.8689
					C21-C22-N27	123.853		121.6545
					C23-C22-N27	113.5205		115.4686
					C22-C23-C24	119.9871		119.4946
					C22-C23-H41	118.7291		119.0972
					C24-C23-H41	121.2742		121.4064
					C23-C24-C25	119.1256		119.364
					C23-C24-H42	120.0061		119.9013
					C25-C24-H42	120.8674		120.7328

					C24-C25-C26	119.8898		120.0531
					C24-C25-H43	120.3603		120.2331
					C26-C25-H43	119.7477		119.7015
					C21-C26-C25	122.8303		122.2458
					C21-C26-H44	118.0976		118.371
					C25-C26-H44	119.0687		119.3779
					C22-N27-O28	117.8031		117.5684
					C22-N27-O29	117.2874		117.0526
					C22-N27-H37	93.5166		95.029
					O28-N27-O29	124.7205		125.3099
					O29-N27-H37	131.5361		129.432
					N18-H37-N27	106.7748		107.7549
					N18-H37-O28	134.1526		135.1026

3.2 IR analysis:

The compound 4M4N2NT has 44 atoms, 204 electrons and 127 modes of vibrations. These vibrational assignments and spectral graph of the compound was examined in both B3LYP/631G and B3LYP/6311G basic sets. This is represented through stretching, bending and vibration deformation and are examined through chemcraft. For visual comparison, the spectral graph and vibrational analysis are given below.

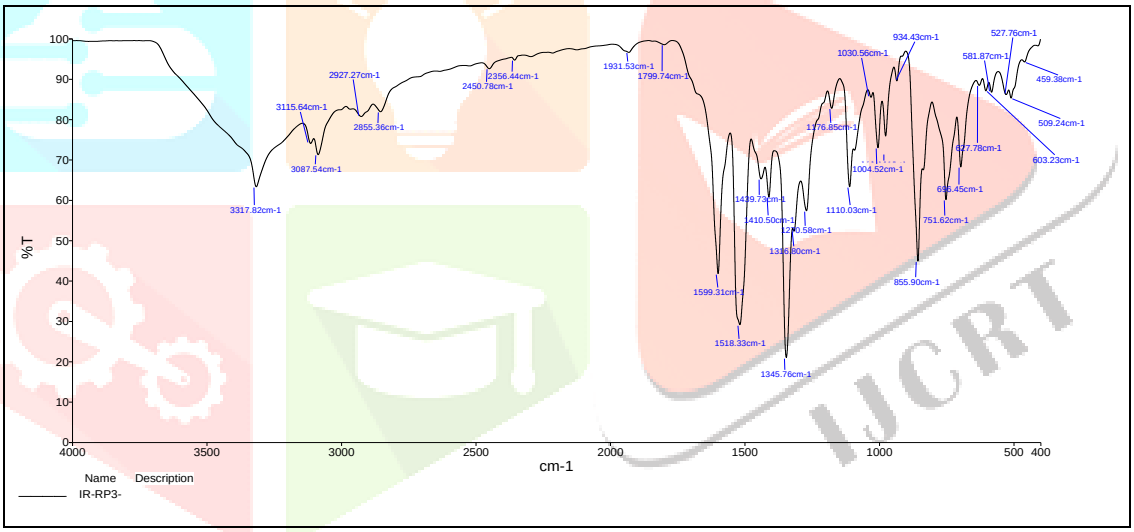

Figure 1. Experimental IR Spectral graph of 4M4N2NT

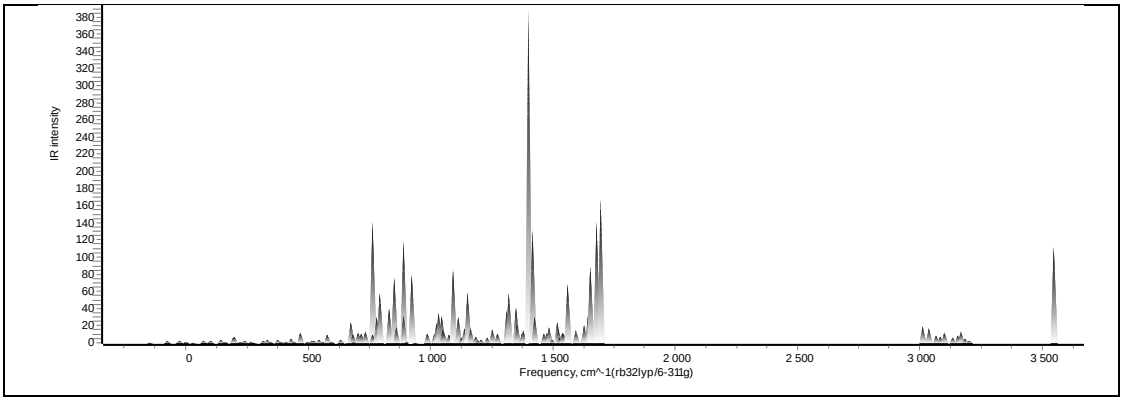

Figure 2. Theoretical IR Spectral graph of 4M4N2NT

N-H Vibration:

The N-H group for the heterocyclic compounds shows bending vibration in the region 1515-1350 cm^{-1} and stretching vibration in region of 3220-3500 cm^{-1} (11-12). For compound 4M4N2NT, the experimental value of N-H stretching vibration is observed at 3317.82 cm^{-1} and the theoretical value peak is observed around 3100-3200 cm^{-1}. The N-H bending for compound A is at 1599.31.

C-H Vibration:

For the aromatic compound, the C-H stretching vibration are observed in region of 2900-3100 cm^{-1} and bending for CH vibration exist in region of 1450-1000 cm^{-1} and 1000-750 cm^{-1} is caused by the out-of-plane and in-plane-bending (13-14). For compound 4M4N2NT, the experimental value of C-H stretching vibration is observed at 3087.54 cm^{-1} and the theoretical value peak is observed around 3000-3100 cm^{-1}. The C-H bending are observed at 1931.53 and 1799.74 cm^{-1}.

C-N Vibration:

Usually the C-N stretching vibration result in the region around 1266-1382 cm^{-1} (15-16). For compound 4M4N2NT, the experimental vibration peak for C-N is observed at 1345.76 cm^{-1} and the theoretical peak for C-N stretching is observed around 1300-1380 cm^{-1}.

N-O Vibration:

The nitro group for the compound 4M4N2NT results as N-O stretching vibration. These N-O stretching vibration of experimental value peak for compound 4M4N2NT is 1518.33 and the theoretical peak is around 1500-1550 cm^{-1}.

3.3 NMR analysis:

The ^{1}H and ^{13}C Nuclear Magnetic Resonance spectra were recorded by Brucker Avance 300 MHz spectrophotometer. The theoretical graph is based on SCF GIAO magnetic shielding method plotted through Gaussian 09W software. The experimental value of ^{1}H and ^{13}C NMR are compared with theoretical value represented in Table 2 and 3. For the compound 4M4N2NT experimental chemical shifts values of aromatic protons were arrived in the region δ 6.0-8.0 ppm. Theoretically the range falls at 6.2 – 7.6 ppm. The methyl protons are arrived at δ 2.631 ppm whereas in the theoretical data three values are arrived for three protons. For equivalent protons there should be one chemical shift value. The stereo chemically non-equivalent CH_2 pyrazoline protons arrived as two doublets of doublet centered at δ 3.077 and δ 3.775 ppm. But theoretically one peak arrived at 2.8152 and the other one taken downfield at 1.1135 ppm. For CH proton, signal arrived as a doublet of doublet centered at δ 5.151. But the theoretical value was 5.021 ppm.

Theoretical and experimental chemical shift values in the ^{13}C NMR spectra of the compound 4M4N2NT is very much consistent other than methyl carbon only. The values are depicted in the table 3.

Table 2. Experimental and theoretical ^{1}H NMR values of 4M4N2NT

^{1}H NMR VALUES (ppm)		
Atoms	Experimental	Theoretical
H30	8.466	8.2811
H31	7.794	7.8071
H32	7.176	7.0469
H33	8.015	8.2442
H34	2.631	1.3124
H35	2.631	1.6856
H36	2.631	1.7013
H37	5.611	5.4503
H38	5.151	4.3154
H39	3.720	2.8152
H40	3.04	1.1135
H41	7.57	7.2803
H42	7.203	7.0878
H43	7.548	7.2725
H44	6.714	6.9373

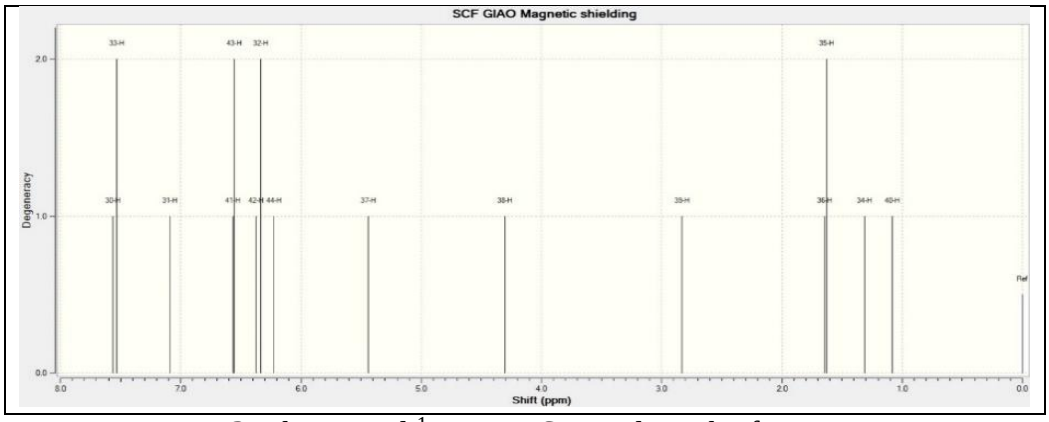

Figure 3. Theoretical ^{1}H NMR Spectral graph of 4M4N2NT

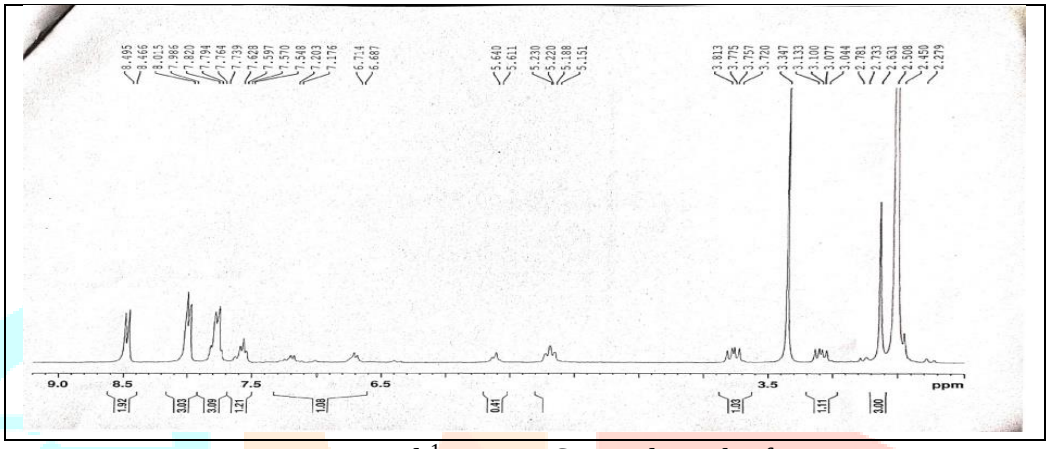

Figure 4. Experimental ^{1}H NMR Spectral graph of 4M4N2NT

Table 3. Experimental and theoretical ^{13}C NMR values of 4M4N2NT

C^{13} NMR VALUES (ppm)		
ATOMS	EXPERIMENTAL	THEORETICAL
C1	148.05	151.03
C2	124.90	128.913
C3	125.57	126.885
C4	143.34	146.885
C5	125.57	128.771
C6	124.96	127.7
C13	140.93	132.138
C14	139.70	135.092
C15	10.55	1.933
C16	114.02	118.259
C19	58.93	55.364
C20	42.74	38.129
C21	127.16	124.266
C22	148.94	139.021
C23	129.03	124.266
C24	126.44	130.58
C25	137.95	135.437
C26	129.16	133.5

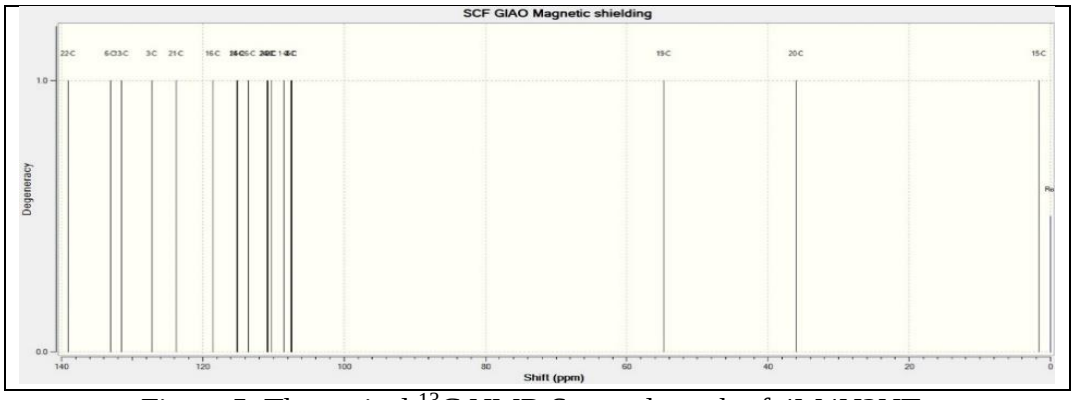

Figure 5. Theoretical ^{13}C NMR Spectral graph of 4M4N2NT

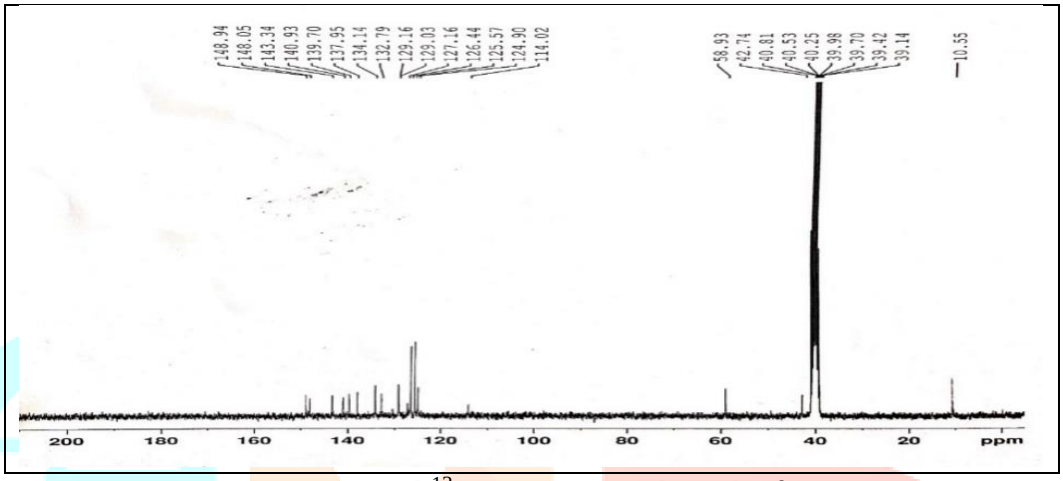

Figure 6. Experimental ^{13}C NMR Spectral graph of 4M4N2NT

3.4 Frontier orbital analysis:

The highest occupied molecular orbital (HOMO) and the lowest unoccupied molecular orbital (LUMO) are called frontier molecular orbitals. The frontier orbital analysis (FMOs) is vital in all the molecules and helps in better understanding of chemical reaction of molecules (17). The electronic properties of electron absorption corresponding to the transition from ground state to first excited state is done by the excitation of one electron between -0.23250 to -0.12099 kcal for compound 4M4N2NT. The smaller the energy gap the higher the stability of molecule. Since the energy gap for compound 4M4N2NT is 0.11151kcal is stable.

In fig 7, the positive phase and negative phase of the compound represented with red and green colour. The energy gap between the HOMO and LUMO indicates the charge transfer interaction within the molecule. The HOMO is electron donor and the energy is related to ionization potential, LUMO related to affinity. The orbital analysis is calculated by b3LYP/631G (d, p).

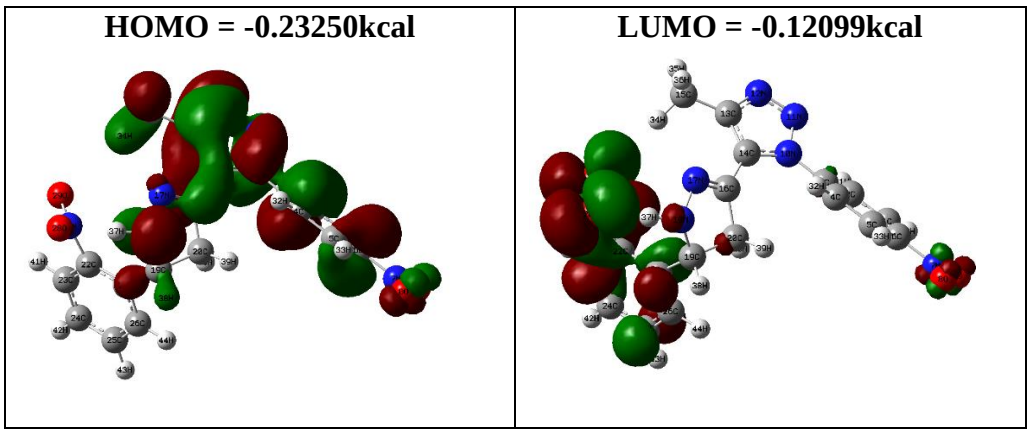

Figure 7. HOMO-LUMO plot of 4M4N2NT

3.5 MEP Analysis:

In molecular modeling calculation, the ESP provides the accurate value of the active site in the molecule (18). The ESP gives the site for nucleophilic and electrophlic bond forming attack, mostly by means of positive and negative region (19). ESP are the group of intersecting sphere where the center are aligned with the nucleus of atom (20). ESP is the density of electron that are external contour of molecule (21). The DFT calculation are carried by B3LYP/631G (d, p) method. The total density energy values for all the compound varies from (-6.164 e^{-2} to +6.164 e^{-2}) and the ESP region energy values for all the compound varies from (-1.637 e^{-2} to +1.637 e^{-2}). The colour red shows the electron rich region and are partially negative, the blue represents the electron defcient region and are partially positive, yellow are slightly electron rich region (22). The positive region are the site for the elctrophilic attack and negative region are the site for nucleophilic attack. The attraction happens in blue region and repultion in orange coloured region (23).

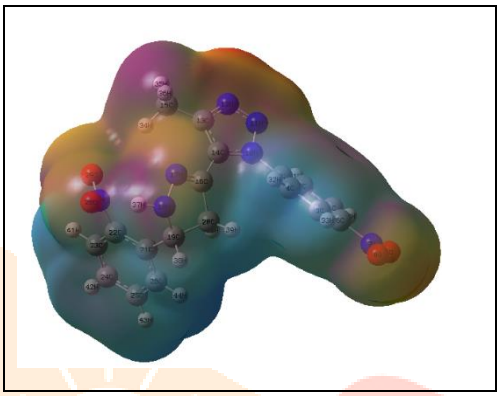

Figure 8. Molecular Electrostatic Potential map of 4M4N2NT

3.6 Mullikan Population Analysis:

The Mullikan analysis represents charge distribution in the molecule (24). The charge value of each atoms is analyzed by this Mullikan population analysis (25). Mullikan charge of compound 4M4N2NT was calculated by B3LYP/631G (d, p) basic set method. This calculated value shows that oxygen atom is delocalized with negative charge value (26). For the compound it shows that O8, O9 that attached with N7 are negative. The N10-N12-N13 in triazole ring also has negative charge value. The positive charge value is observed in the H atoms that are connected with C atoms. Due to diminished electron density higher positive charge is seen on C.

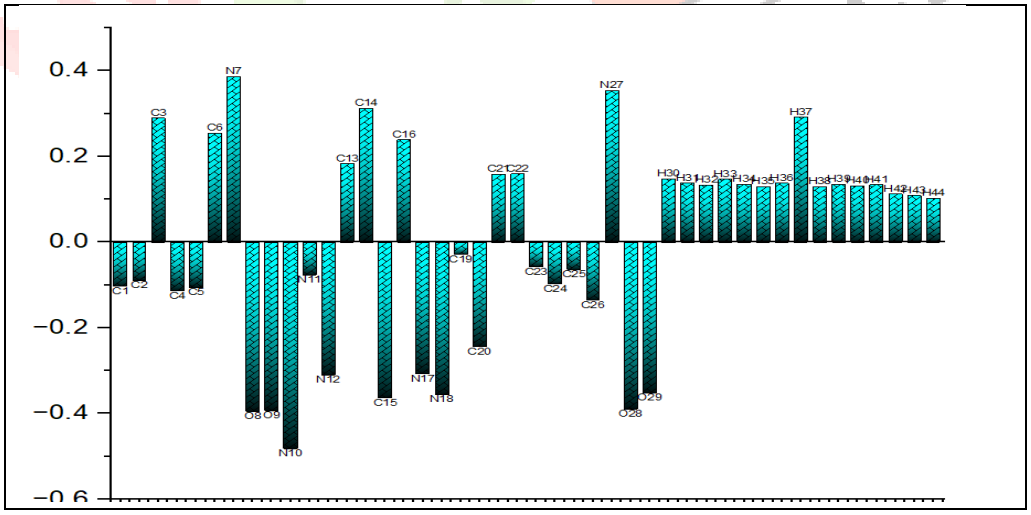

Figure 9. Mulliken charges of 4M4N2NT

3.7 NLO Analysis:

Non-linear optics are measured by the hyperpolarizability and linear polarizability (27) of the molecule. The hyperpolarizability and linear polarizability are in response to applied electric field (28). It determines the strength of molecular interaction, collision process and cross-section of different scattering along with NLO properties (29). The value of hyperpolarizability can get change by the electron correlation (23). To understand the NLO properties, we should understand the intermolecular charge transfer (ICT) between acceptor, donor unit and the properties can vary when there is change in acceptor and donor strength or in

solvent environment (27). When there is higher value of ICT, greater will be NLO values (27). The polarized value is calculated by using B3LYP function with 63IG (d, p) basic set. The total molecular dipole moment of compound 4M4N2NT is shown in table 4.

Table 3. Experimental and theoretical ^{13}C NMR values of 4M4N2NT

Dipole (field-independent basis, Debye):						
X= -3.6581	Y=	-5.5526	Z=	-1.1538	Total=	6.7486
Quadrupole (field-independent basis, Debye-Ang):						
XX= -193.1774	YY=	-172.788	ZZ=	-162.4092		
XY= 21.4407	XZ=	9.2736	YZ=	10.7628		
Traceless Quadrupole (field-independent basis, Debye-Ang):						
XX= -17.0525	YY=	3.3369	ZZ=	13.7156		
XY= 21.4407	XZ=	9.2736	YZ=	10.7628		
Octapole (field-independent basis, Debye-Ang2):**						
XXX= -221.0667	YYY=	-86.2027	ZZZ=	-6.0912	XYY=	-74.1402
XXY= 46.0877	XXZ=	-64.7781	XZZ=	-1.7753	YZZ=	-26.3819
YYZ= 13.046	XYZ=	-3.8911				
Hexadecapole (field-independent basis, Debye-Ang3):**						
XXXX= -13111.7338	YYYY=	-3890.5205	ZZZZ=	-1368.8435	XXXY=	770.527
XXXZ= 156.2394	YYYX=	-109.5885	YYYZ=	192.3219	ZZZX=	0.4504
ZZZY= 30.3241	XXYY=	-2759.9974	XXZZ=	-2085.7672	YYZZ=	-876.792
XXYZ= 129.1547	YYXZ=	85.568	ZZXY=	42.7623		
Exact polarizability:	299.649	-51.55	244.185	-3.783	-7.182	212.2
Approx polarizability:	428.869	397.052	-29.176	-41.836	447.903	

3.8 Contour:

Contour map for a molecule reveals the distribution of electron density (30). From the given fig 9, the yellow surface or line represents positive charge distribution and orange surface represents negative charge distribution (30). In compound 4M4N2NT the region of triazole and nitro group has negative charge distribution. The contour map for compound 4M4N2NT was calculated by using B3LYP/631G (d, p) basic set.

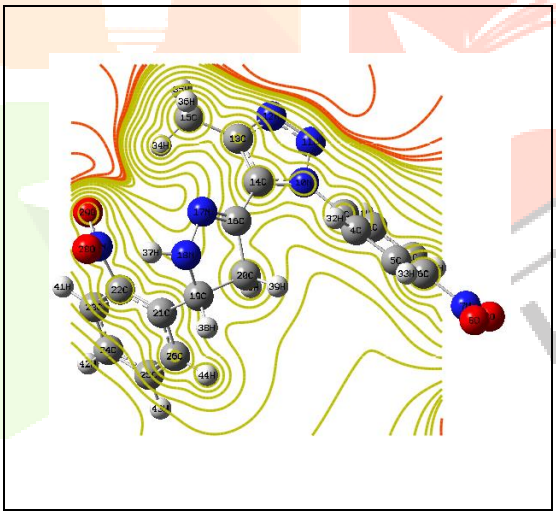

Figure 9. Contour map of 4M4N2NT

IV. Conclusion:

The intricate computational and experimental studies have been carried out on compound 4M4N2NT and the results were disscused. By this study, the experimental and computational value of FT-IR strecthing frequency values and in NMR chemical shift values are found to be in good agreement. The vibrtional spectra for compound 4M4N2NT was proved by the distinctive stretching bands of N-H, N-O, N-N, C-N and C-H groups. The mullikan population analysis shows that nitrogen atom creates more electronegtivity on O8, O9, O28 and O29. The ESP surface study shows the nucleophilic and electrophilic regions. The energy gap for compound 4M4N2NT is 0.11151 kcal. The NLO analysis reveals the dipole moment of the compound as 6.7486. From the acquired results, the vibrational spectra and magnetic resonance chemical shift values are in expected range which confirms the structure of 4-methyl-1-(4-nitrophenyl)-5-5-(2-nitrophenyl)-4-5-dihydro-1H1,2,3 triazole (4M4N2NT).

References:

1. Kumaraswamy, D and Prashanth, D. 2017. Synthesis and Evaluation Of Pyrazoline Derivatives As Antibacterial Agents, International Journal of Pharmacy and Biologic, 7(1):84-93.

2.Suresh Kumar, Sandhya Bawa, Sushma Drabu, Rajiv Kumar and Himanshu Gupta. 2009. Biological Activities of Pyrazoline Derivatives -A Recent Development, Recent Patents on Anti-Infective Drug Discovery, 4:154-163.

3. Mohamed R Shaaban, Abdelrahman S Mayhoub and Ahmad M Farag. 2012. Recent advances in the therapeutic applications of pyrazolines, Expert Opinion on Therapeutic Patents, 22(3):253-291.

4. Aftab Ahmad, Asif Husain, Shah Alam Khan, Mohd. Mujeeb, Anil Bhandari. 2014. Synthesis, antimicrobial and antitubercular activities of some novel pyrazoline derivatives, Journal of Saudi Chemical Society, 41(5).

5. Ahmet Ozdemir. 2013. Synthesis and antimicrobial activity of some pyrazoline derivatives bearing amide moiety, Marmara Pharmaceutical Journal 17:187-192.

6. Kosrat N. Kaka, Salam G. Taher, Wali M. Hamad and Aram H. Ibrahim. 2019. Synthesis of new series of Pyrazoline, and study their Kinetics and Reaction Mechanism, ARO-The Scientific Journal of Koya University 7(2):5-13.

7. Suvitha, A Periandy, S Gayathri, P. 2014. NBO, HOMO-LUMO, UV, NLO, NMR and vibrational analysis of veratrole using FT-IR, FT -Raman, FT-NMR spectra and HF - DFT computational methods, Spectrochimica Acta Part A Molecular and Biomolecular Spectroscopy, 138C:357-369

8. Carthigayan, K Xavier, S Periandy, S. 2015. HOMO–LUMO, UV, NLO, NMR and vibrational analysis of 3-methyl-1-phenylpyrazole using FT-IR, FT-RAMAN, FT-NMR spectra and HF-DFT computational methods, Spectrochimica Acta Part A: Molecular and Biomolecular Spectroscopy, 142:350–363.

9. Camargo, A J Napolitano, H B Zukerman-Schpector, J. 2007. Theoretical investigation of the intramolecular hydrogen bond formation, non-linear optic properties, and electronic absorption spectra of the 8-hydroxiquinoline, Journal of Molecular Structure: THEOCHEM, 816:145–151.

10. Philippe d'Antuono, Edith Botek, Benoît Champagne, Milena Spassova, and Pavletta Denkova, 2006. Theoretical investigation on and NMR chemical shifts of small alkanes and chloroalkanes, J. Chem. Phys. 125, 144309.

11. Gunasekaran, S Kumaresan, S Arun Balaji, R Anand, G Seshadri, S. 2008. Vibrational Spectra and Normal Coordinate Analysis on Structure of Chlorambucil and Thioguanine, Pramana – Journal of Physics, 71:1291-1330.

12. Gunasekaran, S Arun Balaji, R Kumaresan, S Anand, G Vivekanand, M. 2009. Computation and interpretation of vibrational spectra on the structure of Nitrazepam using semi-empirical and density functional methods, International Journal of ChemTech Research, 1(4):1109-1124.

13. Gunasekaran, S Kumaresan, S Seshadri, S Muthu, S. 2008. Vibrational spectra and normal coordinate analysis of structure of procarbazine, Indian Journal of Pure & Applied Physics, 46:155-161.

14. Gunasekaran, S Arun Balaji, R Kumaresan, S Seshadri, S Muthu, S. 2008. Vibrational spectral assignments of paraldehyde by ab initio and density functional methods, Journal of Molecular Modeling 14:375-383.

15. Gunasekaran, S Kumaresan, S Arun Balaji, R Anand, G Srinivasan, S. 2009. Density functional theory study of vibrational spectra, and assignment of fundamental modes of dacarbazine, Journal of Chemical Science 120(3):315-324.

16. Gunasekaran, S Sailatha, E Seshadri, S Kumaresan, S. 2009. FTIR, FT Raman spectra and molecular structural confirmation of isoniazid, Journal of Pure & Applied Physics 47:12-18.

17. Selvaraj, S Rajkumar, P Kesavan, M Mohanraj, K Gunasekaran, S Kumaresan, S. 2018. A combined experimental and theoretical study on 4-hydroxy carbazole by FT-IR, FT-Raman, NMR, UV–visible and quantum chemical investigations, Chemical Data Collections, 17:302-311.

18. Ahmed M. Bayoumy, Medhat Ibrahim, Amina Omar. 2020. Mapping molecular electrostatic potential (MESP) for fulleropyrrolidine and its derivatives, Optical and Quantum Electronics, 52:346.

19. Felipe A. Bulat & Alejandro Toro-Labbé & Tore Brinck & Jane S. Murray & Peter Politzer. 2010. Quantitative analysis of molecular surfaces: areas, volumes, electrostatic potentials and average local ionization energies, J Mol Model, 16:1679–1691.
20. Chengteh Lee, eitao Yang and Robert G. Parr. 1988. Physical Review, 8:37.
21. Bader, R F W Henneker, W H and Paul E. Cade. 1967. Molecular Charge Distributions and Chemical Binding, J. Chem. Phys. 46:3341.
22. Govindasamy, P Gunasekaran, S Srinivasan, S. 2014. Molecular geometry, conformational, vibrational spectroscopic, molecular orbital and Mulliken charge analysis of 2-acetoxybenzoic acid, Spectrochimica Acta Part A: Molecular and Biomolecular Spectroscopy, 130:329–336.
23. Muthu, S Elamurugu Porchelvi. E. 2013. FTIR, FT-RAMAN, NMR, spectra, normal co-ordinate analysis, NBO, NLO and DFT calculation of N,N-diethyl-4-methylpiperazine-1-carboxamide molecule, Spectrochimica Acta Part A: Molecular and Biomolecular Spectroscopy, 115:275-286.
24. Govindarajan, M Karabacak, M. 2012. Spectroscopic properties, NLO, HOMO-LUMO and NBO analysis of 2,5-Lutidine, Spectrochimica Acta Part A: Molecular and Biomolecular Spectroscopy, 96:421–435.
25 Murali, M K and Balachandran, V. 2012. FT-IR, FT-Raman, DFT structure, vibrational frequency analysis and Mulliken charges of 2-chlorophenylisothiocyanate, Indian journal of pure & applied physics, 50(1):19-25.
26. Govindasamy, P Gunasekaran, S Srinivasan, S. 2014. Molecular geometry, conformational, vibrational spectroscopic, molecular orbital and Mulliken charge analysis of 2-acetoxybenzoic acid, Spectrochimica Acta Part A: Molecular and Biomolecular Spectroscopy, 130:329-336.
27. Prerana K M. Lokhande, Dinesh S. Patil, Mayuri M Kadam and Nagaiyan Sekar. 2019. Theoretical Investigation of Optical and Nonlinear Optical (NLO) Properties of 3 - Azabenzanthrone Analogues: DFT and TD - DFT Approach, Electro, Physical & Theoretical Chemistry, 4:10033-10045.
28. Zeynep Demircioglu, Gokhan Kastas, Çigdem Albayrak Kastas, Rene Frank. 2019. Spectroscopic, XRD, Hirshfeld surface and DFT approach (chemical activity, ECT, NBO, FFA, NLO, MEP, NPA& MPA) of (E)-4-bromo-2-[(4-bromophenylimino)methyl]-6-ethoxyphenol, Journal of Molecular Structure, 1191:129-137.
29. Shimaa Abdel Halim, Magdy A. Ibrahim, Synthesis. 2017. DFT calculations, electronic structure, electronic absorption spectra, natural bond orbital (NBO) and nonlinear optical (NLO) analysis of the novel 5-methyl-8H-benzo[h]chromeno[2,3-b][1,6] naphthyridine-6(5H),8-dione (MBCND), Journal of Molecular Structure,1130(15):543-558.
30. Zahra Nikfar, Zahra Shariatinia. 2017. DFT computational study on the phosphate functionalized SWCNTs as efficient drug delivery systems for anti-osteoporosis zolendronate and risedronate drugs, Physica E: Low-dimensional Systems and Nanostructures, 91:41-59.